Oxygen isotopes reveal glacial-interglacial changes in the timing of pedogenic carbonate growth from the Chinese Loess Plateau

Jiawei Da[1*, 2], Gen K. Li[3], Junfeng Ji[1]

[1] Key Laboratory of Surficial Geochemistry, Ministry of Education, School of Earth Sciences and Engineering, Nanjing University, 210023 Nanjing, China.

[2] Frontiers Science Center for Critical Earth Material Cycling, Nanjing University, 210023 Nanjing, China

[3] Department of Earth Science, University of California, Santa Barbara, CA 93106, USA

Corresponding author: Jiawei Da (dajiawei@nju.edu.cn)

Key Points: (140 characters each)

- Modern observations and modeling efforts delineate the seasonality of pedogenic carbonates on the Chinese Loess Plateau.
- The ^{18}O of pedogenic carbonates show opposite correlations with rainfall proxies for glacial and interglacial samples.
- Rainfall-induced changes in the seasonality of pedogenic carbonate growth explain the nonunique ^{18}O-rainfall patterns.

Abstract (150 words)

Pedogenic carbonates document a wealth of environmental information, but their seasonal variations may obscure long-term trends. Here we report evidence of changing seasonality of pedogenic carbonate growth from the Chinese Loess Plateau during the Quaternary glacial cycles, using the ^{18}O of pedogenic carbonates ($^{18}O_c$). The glacial and interglacial $^{18}O_c$ show negative and positive correlations with proxy-inferred rainfall amount, respectively. We explain this pattern using modern observations and modeling results, which show opposite correlations between $^{18}O_c$ and rainfall amount in growing versus non-growing seasons. In glacial episodes under weak monsoon, pedogenic carbonate growth occurred within the growing season, inheriting a negative $^{18}O_c$-rainfall correlation. Conversely, pedogenic carbonate growth likely extended into the non-growing season during interglacials due to intensified monsoonal rainfall, incorporating a positive $^{18}O_c$-rainfall correlation. Our work links seasonal fluctuations of pedogenic carbonates with their long-term records, shedding new light on interpreting this paleoarchive.

Plain Language Summary

Secondary carbonates in fossil soils are widely used to infer past changes in regional ecology and hydrology at annual-to-multi-year resolutions. However, these records can be biased by intra-annual, seasonal variabilities. Modern soil studies indicate variable seasonal distributions of soil carbonate formation under

different climate conditions. This study examines the effect of carbonate formation timespans on the long-term records derived from the Pleistocene paleosols collected from the Chinese Loess Plateau, using oxygen isotopic compositions of soil carbonates ($^{18}O_c$). Our records show a positive correlation between $^{18}O_c$ and rainfall amount during interglacial periods and a negative correlation during glacials. Corroborated by modern observations and numerical modeling, we propose that changes in carbonate-formation seasons can explain the diverse glacial-interglacial $^{18}O_c$ - rainfall patterns. Our results highlight the importance of soil carbonate seasonality when using this archive for paleoenvironmental reconstructions.

1. Introduction

Secondary carbonates formed during pedogenesis (pedogenic carbonates) are a common terrestrial archive for reconstructing long-term environmental changes (Zamanian et al., 2016). For instance, the carbon isotopic compositions of pedogenic carbonates ($^{13}C_c$) document past changes in atmospheric CO_2 levels, aboveground vegetation biomes, and soil productivity (Cerling et al., 2011; Da et al., 2019; Licht et al., 2020). The triple-oxygen and clumped isotopic compositions of pedogenic carbonates record soil temperature and evaporation intensity (Beverly et al., 2021; Kelson et al., 2020). Other studies show that the oxygen isotopic compositions of pedogenic carbonates ($^{18}O_c$) inherit the ^{18}O of soil water and reveal regional hydrology (Caves & Chamberlain, 2018).

Although pedogenic carbonates are widely used to reconstruct past environmental records from millennial to million-year timescales (Caves et al., 2016), their seasonal variability and related influence on the long-term records remain less well understood (Breecker et al., 2009; Yang et al., 2012). The precipitation of pedogenic carbonates from soil solution depends on multiple environmental factors, including rainfall, soil temperature, and soil pCO_2 (Drever, 1982). The seasonal patterns of those factors vary under different climate regimes and can cause changes in the seasonality of pedogenic carbonate growth (Breecker et al., 2009; Huth et al., 2019). Moreover, the isotopic compositions of pedogenic carbonates (e.g. $^{13}C_c$ and $^{18}O_c$) are governed by seasonally variable factors (e.g. soil productivity, temperature, and the ^{18}O of local meteoric water, $^{18}O_p$) (Breecker et al., 2009; Caves & Chamberlain, 2018), suggesting seasonal fluctuations in those isotopic signals as well. Understanding the seasonality of pedogenic carbonates and how the seasonality translates into annual-to-multi-year signals is thus of critical importance for interpreting records and developing proxies from this archive.

The Chinese Loess Plateau (CLP) provides a unique setting to study the seasonality of pedogenic carbonates. The East Asian summer monsoon dominates the regional climate, introducing seasonal wet-dry cycles that facilitate the growth of pedogenic carbonates (Meng et al., 2018). Meteorological data and paleo- ^{18}O records (e.g. from speleothem and microcodium) suggest that in the summer monsoon region, an intensified monsoonal rainfall tends to produce lower $^{18}O_p$

because the Rayleigh distillation process preferentially removes ^{18}O from water vapor (Wang et al., 2008; Zhang et al., 2018). However, the paleosol $^{18}O_c$ from the CLP often increases with bulk soil magnetic susceptibility (MS) – a standard proxy for the summer monsoon intensity (Ding & Yang, 2000; Dong et al., 2018), meaning higher $^{18}O_c$ under enhanced rainfall.

The positive correlation between paleosol $^{18}O_c$ and rainfall amount on the CLP may be related to the seasonality of pedogenic carbonates (Yang et al., 2012). Modern $^{18}O_p$ and rainfall amount have opposite trends in wet versus dry seasons in the summer monsoon region caused by different $^{18}O/^{16}O$ fractionations during the Rayleigh distillation and re-evaporation (Araguás-Araguás et al., 1998; Dansgaard, 1964; Lee et al., 2012). Recent observations and modeling studies indicate that rainfall events govern pedogenic carbonate formation timespan in modern soils (Huth et al., 2019; Kelson, 2019). Based on the spatial patterns of ^{13}C and ^{18}O of calcite nodules across the CLP over the last three interglacial episodes, Yang et al. (2012) suggested that the timing of carbonate formation likely responds to rainfall patterns with a longer period under intensified monsoon. However, a systematic evaluation of pedogenic carbonate seasonality across modern, glacial, and interglacial timescales is still missing.

To better understand the seasonality of pedogenic carbonates on the CLP and its influence on long-term records, we focus on paleosol $^{18}O_c$ systematics combining modern observations, modeling efforts, and examination of Quaternary records. We first model carbonate ^{18}O and growth histories on the CLP, and then identify the influence of pedogenic carbonate seasonality in Quaternary paleosol $^{18}O_c$ records. Our results indicate that the seasonality of pedogenic carbonate systems can translate into the variable correlations between ^{18}O and summer monsoon proxies, which in turn can be used to identify pedogenic carbonate seasonality in paleosols.

2. Materials and Methods

2.1. Modeling the ^{18}O and growth history of pedogenic carbonates

To estimate $^{18}O_c$ under given environmental conditions on the CLP, we adopted a semi-mechanistic isotope model, which has successfully reproduced $^{18}O_c$ of Holocene pedogenic carbonates formed under various climate regimes (Fischer-Femal & Bowen, 2021). The model accounts for multiple processes that could fractionate the $^{18}O/^{16}O$ of soil water, such as the mixing of seasonal rainfall with distinct $^{18}O_p$, and the evaporation and diffusion of water molecules. We applied this model to modern soil systems on the CLP using monitored temperature, precipitation, and $^{18}O_p$ data from Global Network of Isotopes in Precipitation (GNIP) stations (https://nucleus.iaea.org/wiser/index.aspx) (Figure 1a), and calculated theoretical $^{18}O_c$ values during both the wet/growing (June, July, August, September) and dry/non-growing (March, April, October, November) seasons (details in Text S1 and Table S1). We then compared the modeled $^{18}O_c$ to the measured $^{18}O_p$ for different seasons.

To explore the seasonality of pedogenic carbonate growth, we simulated the dissolution and precipitation of calcites within a 1D soil column (100 cm), using a numerical model of soil physics and carbonate chemistry (HYDRUS-1D) (Simunek et al., 2005). This model has successfully simulated vadose zone hydrology and carbonate chemistry in modern soils (Kelson, 2019; Meyer et al., 2014). We run daily simulations for a whole year, with boundary conditions (e.g. precipitation, temperature, vegetation density) constrained by meteorological data retrieved from the Lantian County located on the southern edge of the CLP (see Text S2 and Data Set S1).

2.2. Sampling and analyzing Quaternary loess-paleosol sequences

2.2.1. Sampling and chronology

To understand pedogenic carbonate seasonality over the Quaternary glacial-interglacial cycles, we collected paleosol samples from two loess-paleosol sequences (ZJC and FX) located at the central CLP (Figure 1a). The Quaternary loess-paleosol sequences developed on the continuous eolian deposits, with alternating paleosol units (S_i, dark brown) formed during the interglacial episodes and the loess units (L_i, light yellow) formed during the glacial episodes (An et al., 2014).

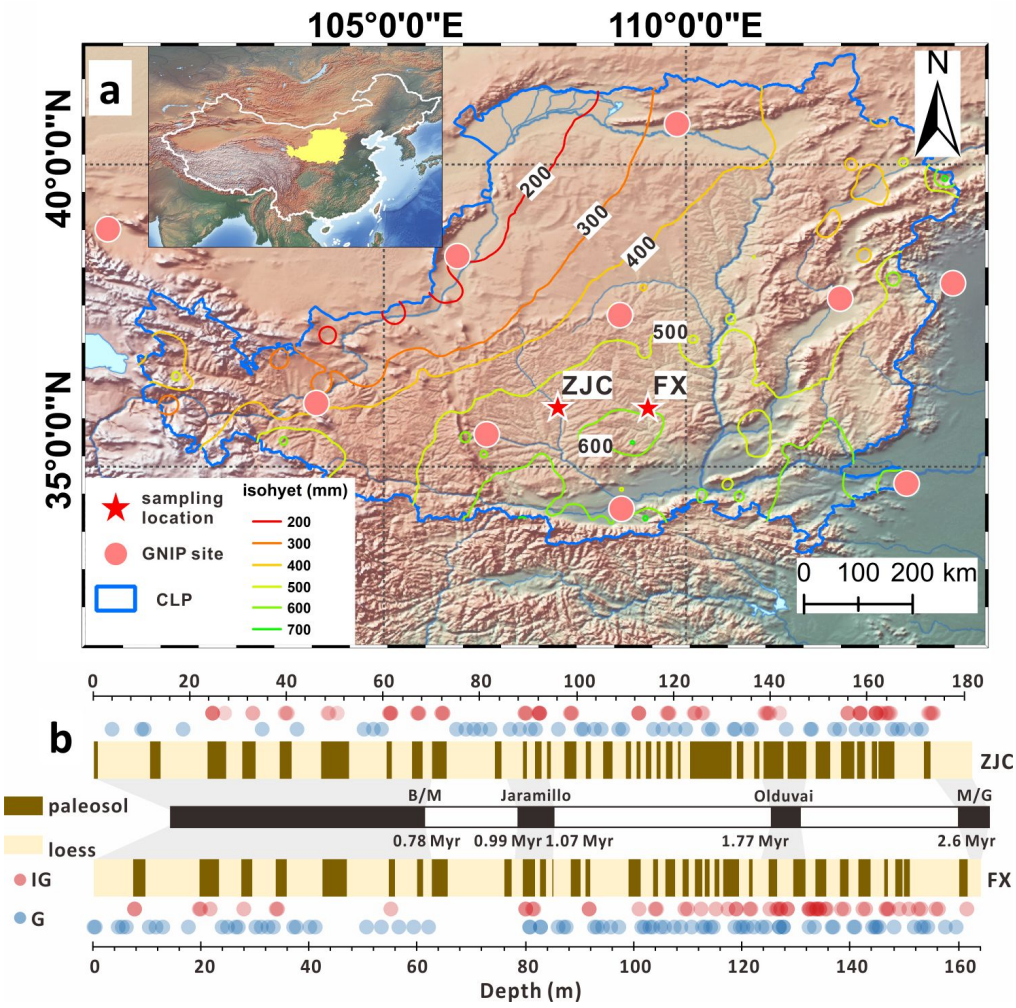

Figure 1. Settings and sampling site information. (a) Map showing the location of the Chinese Loess Plateau (yellow area in the insert), the sampling sites (red stars), and the GNIP sites (circles). (b) Stratigraphic columns showing the sampling soil units, with the colored symbols denoting the loess and paleosol units and the corresponding interglacial (IG) and glacial (G) samples.

For the FX section, a 206-m drilling core was retrieved from the highest terrace near Fuxian County (N 36°9 33 E 109°27 6), with the upper 161.7-m being the Quaternary loess-paleosol sequence. Bulk soil samples were then collected at 2-cm intervals for subsequent analyses in the laboratory. For the ZJC section (N 35°46 38 E 107°47 25), bulk soil samples were collected from the fresh exposure of trenched soil profiles at 10-cm intervals. All the bulk samples were measured for MS to constrain chronology. For MS measurements, approximately 10 g of bulk paleosol samples were ground into powder, oven-dried, and analyzed

on a Bartington MS2 system with a 5% accuracy. The ages of our studied loess-paleosol sequences are established by MS chronostratigraphy concerning the Lingtai section, the chronology of which was determined by paleomagnetic polarity and astronomical tuning (Sun et al., 2006).

We also measured the carbonate contents of bulk soil samples, a typical summer monsoon proxy (Meng et al., 2018), through Fourier transform infrared spectroscopy (FTIR) using a Thermo Scientific Nicolet 6700 spectrometer, following published protocols (Meng et al., 2015).

2.2.2. Sample treatments

We focus on finely disseminated calcites (FDC) in bulk paleosols (Da et al., 2019), which are characterized by needle-fiber-shaped calcite crystals ranging in sizes from nanometers to micrometers (Barta, 2011). Based on geochemical analyses, previous studies have confirmed that these calcites are of pedogenic origin (Da et al., 2019) and can be used for paleoenvironmental reconstructions (Milliere et al., 2011). Notably, the parent material of the loess contains carbonate minerals including both calcite and dolomite (Meng et al., 2015), the incomplete dissolution of which could introduce considerable noise to the stable isotope signals. To avoid detrital contamination, we treated samples following the criteria below.

For the interglacial paleosol layers, we selected bulk paleosol samples devoid of dolomite, as evidenced by FTIR analysis (Meng et al., 2015). Because pedogenesis developed on the loess only produces calcite, and since dolomite dissolves much slower than calcite, its disappearance suggests a complete dissolution of detrital carbonate (Meng et al., 2015). However, this practice cannot be applied to the loess layers, in which dolomite remains due to low rainfall in the glacials (Meng et al., 2018). Instead, we separated the clay-sized fractions (<2um) from bulk paleosols following a centrifugal-separation method (Zhao et al., 2015). The clay-sized fractions are thought to be dominated by authigenic carbonates because the dissolution-precipitation process preferentially occurs in fine-grained carbonates (Hu et al., 2018; Sheng et al., 2008).

2.2.3. Analyses

To evaluate the seasonal variations of pedogenic carbonate isotopic signals and their relations with the rainfall amount, we measured the ^{13}C and ^{18}O of the FDC in the selected samples as $^{13}C_c$ and $^{18}O_c$. We also measured the trace elements in the acid-soluble fractions to characterize the geochemical compositions of the FDC. Detailed analytical procedures and data are provided in Text S3 and Data Set S2, respectively.

3. Results and Discussion

3.1. Seasonality in pedogenic carbonates from modern observations

In this section, we report modern observations and modeling results to demonstrate a strong seasonality in pedogenic carbonate systems on the CLP and how this seasonality translates into the $^{18}O_c$-rainfall amount relations.

3.1.1. Rainfall $^{18}O_p$ as a primary control on pedogenic carbonate $^{18}O_c$

Previous studies consider that $^{18}O_c$ is dominated by local $^{18}O_p$, with other environmental factors such as temperature and evapotranspiration processes imposing minor effects (Cerling & Quade, 1993; Yang et al., 2012). On the CLP, the ^{18}O and D of soil water collected from modern soil profiles correlate tightly with those of rainfall water (Lyu et al., 2021) (Figure S1), corroborating a dominant role of $^{18}O_p$ in setting $^{18}O_c$. The output $^{18}O_c$ from the semi-mechanistic isotope model also show high correlations with the input $^{18}O_p$ (Figures 2a-2b), further supporting a primary control of $^{18}O_p$ on $^{18}O_c$. Based on the field data and modeling results, we propose that the variations in the $^{18}O_c$ from the Quaternary paleosols should closely track those of the rainfall $^{18}O_p$.

3.1.2. Pedogenic carbonate seasonality revealed by rainfall-^{18}O relationships

Mean annual precipitation (MAP) and seasonal $^{18}O_p$ data from the GNIP sites across the CLP show opposite trending patterns during the growing and non-growing seasons (Figures 2c-2d). These patterns are consistent with the coastal-to-inland $^{18}O_p$ trends in wet versus dry seasons in the East Asian summer monsoon domain (Araguás-Araguás et al., 1998). In the dry/non-growing season, the Rayleigh distillation process leads to decreased $^{18}O_p$ with reduced rainfall along the coast-to-inland trajectory (Dansgaard, 1964). In the wet/growing season, the re-evaporation of raindrops through the dry air likely plays a more important role, which enriches ^{18}O and increases $^{18}O_p$ from the coast to the inland region (Lee et al., 2012). The $^{18}O_p$-MAP and $^{18}O_p$- $^{18}O_c$ relationships (Figure 2) mean that the $^{18}O_c$-rainfall relationship is sensitive to the formation timespan (growing versus non-growing seasons) of pedogenic carbonate.

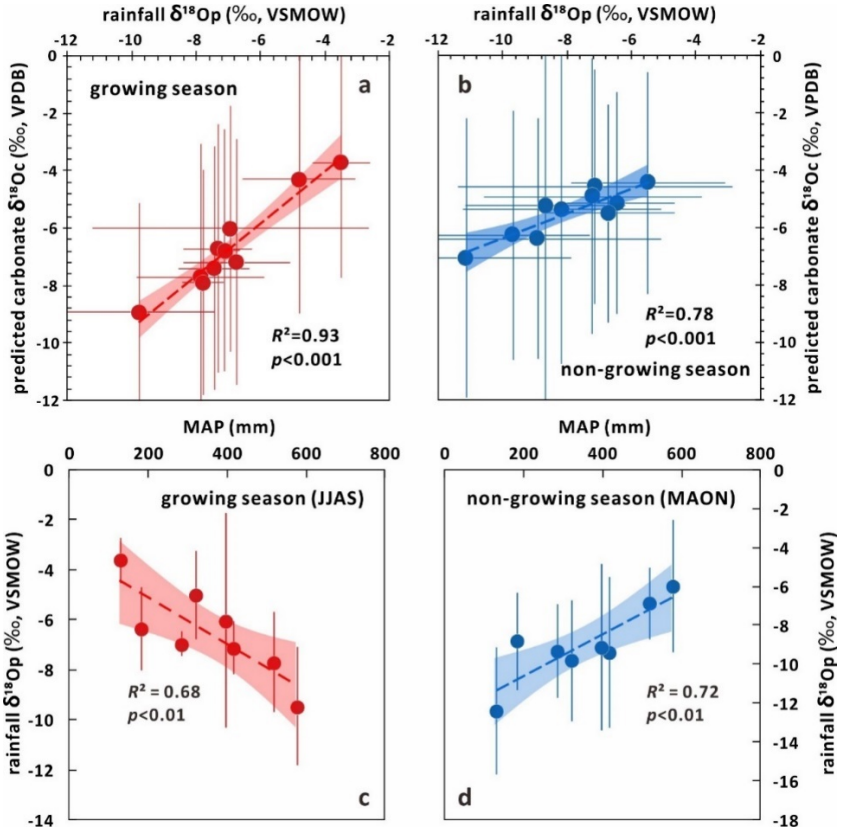

Figure 2. Relationships between the rainfall amount and ^{18}O of rainfall and pedogenic carbonate. (a-b) rainfall $^{18}O_p$ versus modeled $^{18}O_c$ values using the isotope model from Fischer-Femal and Bowen (2020) (X-axis error bars: 1 measurement errors, Y-axis error bars: 1 uncertainties of the modeled results). (c-d) The modern MAP- $^{18}O_p$ relationships during the growing and non-growing seasons (data from GNIP, error bars: 1 measurement errors). All dashed lines indicate the least-squares regression lines, and the shaded areas show 95% confidence intervals.

Although pedogenic carbonates are thought to form in the growing season (e.g. Cerling, 1999), two mechanisms likely explain pedogenic carbonate formation in the non-growing season. First, an intensified summer monsoon causes more rainfall events in the non-growing season (Figure S2), facilitating infiltration and altering carbonate-system chemistry in soil solutions to precipitate carbonates (Yang et al., 2012). Second, newly formed calcites comprise the outermost layer of pedogenic carbonates (Huth et al., 2019), making them preferentially dissolved in later rainfall events. Consequently, pedogenic carbonates formed in the growing season may get dissolved and reprecipitated in the later non-growing season. Consequently, the $^{18}O_c$ can mix signals from both growing and non-growing seasons, leading to variable $^{18}O_c$-rainfall relations.

3.1.3. Pedogenic carbonate seasonality explored using solute transport modeling

Based on the numerical modeling approach (HYDRUS-1D), previous work simulated soil carbonate accumulation using meteorological data measured from New Mexico, USA (Kelson, 2019). Their results show that 1) changes in the rainfall distribution pattern affect the timing of pedogenic carbonate growth; 2) asynchronous calcite accumulation at various depths owing to differences in soil CO_2, temperature, and water content. To further examine pedogenic carbonate seasonality on the CLP, we modeled changes in calcite concentrations at various soil depths, with input boundary conditions constrained by local meteorological data.

Our modeling results show sizable accumulations of calcites occurring immediately after major rainfall events (Figure 3), confirming a fundamental role of rainfall infiltration in setting soil carbonate chemistry (Huth et al., 2019). Moreover, owing to the differences in soil CO_2, temperature, and soil water $[Ca^{2+}]$ (Figure S3), the timing of carbonate accumulation varies at different depths (Figures 3b-3d), consistent with modern soil observations (Ringham et al., 2016).

The modeling results illustrate a detailed history of carbonate formation (Figure 3). During earlier rainfall events, carbonate minerals at shallow depths are completely leached (Figure 3a), making the percolating soil solution produced in later rainfall events undersaturated in $[Ca^{2+}]$ when reaching the upper part of the carbonate accumulation horizon (Bk horizon). The $[Ca^{2+}]$-unsaturated solution then dissolves calcites formed earlier at the top of the Bk horizon, resulting in substantial calcite accumulation during the non-growing season (Figure 3b). When moving downward into the Bk horizon, the soil solution becomes gradually $[Ca^{2+}]$-supersaturated, precipitating calcites without dissolving previously formed ones from the corresponding depth, thus a consistent accumulation after each rainfall event (Figure 3c). As most calcites precipitate in the middle part of the Bk horizon (Figure 3c), newly formed calcites at deeper depth are slightly more than the dissolved ones after each rainfall event (Figure 3d), thus carrying multi-season $^{18}O_p$ signals. The modeling results add to the proposed mechanisms of carbonate formation in non-growing seasons (Section 3.1.2) and provide insights into how non-growing-season $^{18}O_p$ signals incorporate into the $^{18}O_c$ signals under intensified monsoon.

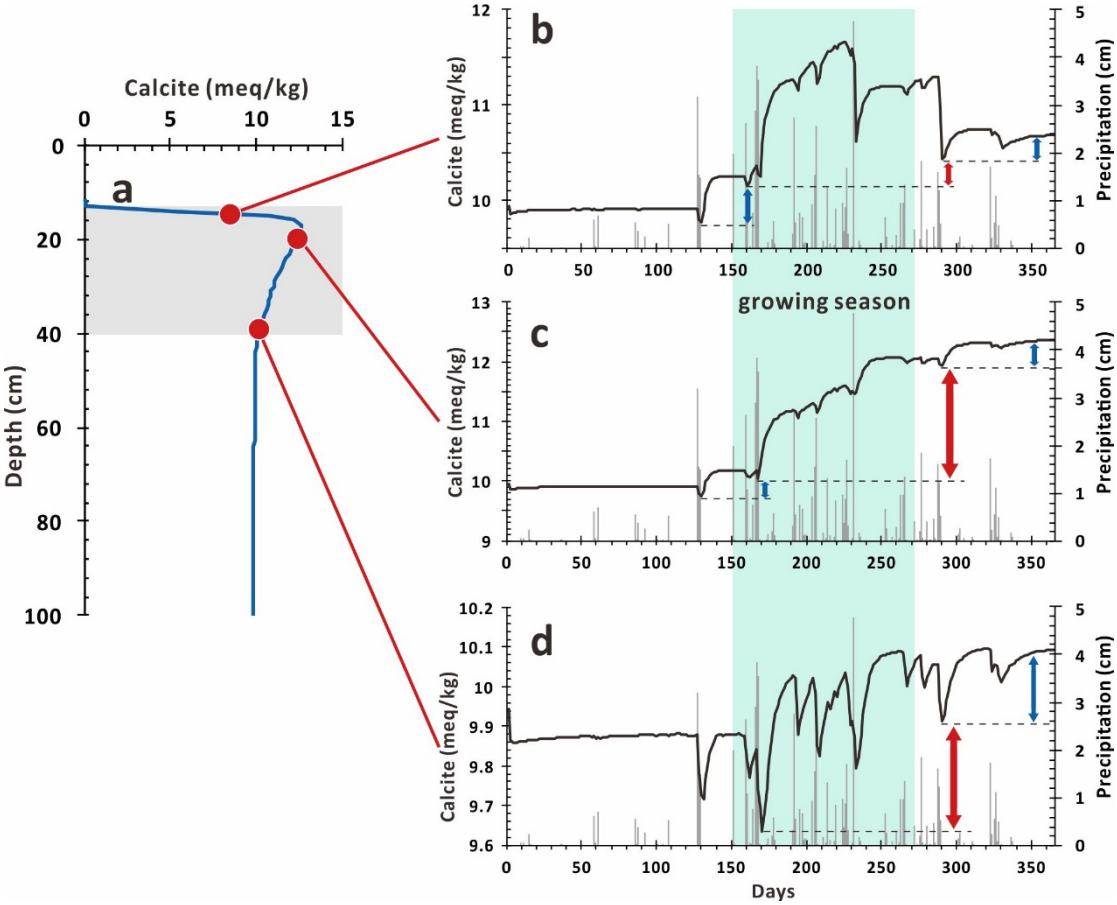

Figure 3. Simulated calcite growth dynamics within a soil column. (a) The distribution of calcite with depth after the one-year simulation, with the Bk horizon highlighted by the grey shade. (b-d) Calcite dissolution and precipitation at various depths (black) in response to rainfall events (grey). Red and blue arrows denote calcite growth at the growing and non-growing seasons. The green shade marks the growing season.

3.2. Pedogenic carbonate seasonality revealed in Quaternary $^{18}O_c$ records

Our modeling results indicate that pedogenic carbonates can form in and integrate $^{18}O_p$ signals from both growing and non-growing seasons, leading to variable $^{18}O_c$-rainfall relationships. In this section, we test whether such seasonality translates into the long term by examining Quaternary $^{18}O_c$ records from the CLP (Figures 1b and S5). We first validate that our analyzed calcite samples are purely pedogenic and then examine the relations between $^{18}O_c$ and monsoon-intensity proxies.

3.2.1. Pedogenic origin of fine-grained calcites

Several lines of evidence suggest that our selected samples (the dolomite-free, interglacial bulk soil samples, and the clay-sized fractions of glacial soil samples) do not contain detrital carbonates. First, the scanning electron microscopy imaging shows that needle-fiber-shaped calcite crystals are the dominant morphology of carbonate minerals (Figure S4), consistent with previous studies (Da et al., 2019; Wang et al., 2022). These calcites represent typical authigenic carbonates formed in loess-parented soils (Barta, 2011).

Second, the geochemical characteristics of the carbonate samples also support a minor contribution from detrital carbonates. The Sr/Ca ratios of the FDC in the interglacial samples (0.9 ± 0.3 mmol/mol, n=80) and glacial samples (0.8 ± 0.3 mmol/mol, n=121) are similar to those in microcodiums (1.1 ± 0.6 mmol/mol, n=15) - a typical secondary carbonate in loess (Li & Li, 2014). The Mg/Ca ratios (82 ± 35 mmol/mol for interglacial samples and 83 ± 38 mmol/mol for glacial samples) are significantly lower than those of detrital carbonates from potential source regions (341 ± 81 mmol/mol, n=19) (Figure S5), which is consistent with the expected behaviors of Mg in carbonate minerals considering its low partition coefficients (Li et al., 2013). The $^{13}C_c$ of these FDC (~-8‰ to -4‰) are consistent with those of coeval calcite nodules (~ -9‰ to -6‰) – another typical type of pedogenic carbonates (Da et al., 2015, 2020) and are significantly lower than those of detrital carbonates (~0‰) (Li et al., 2013).

3.2.2. $^{18}O_c$-rainfall patterns in the Quaternary records

Our studied sections (ZJC and FX, Figure 1) show overlapping distributions of glacial and interglacial $^{18}O_c$, with no apparent long-term trends over the Quaternary glacial cycles (Figure S6). Mean interglacial $^{18}O_c$ values from both sections (ZJC: -9.0±0.4‰, n=84; FX: -9.0±0.4‰, n=59) are slightly higher than glacial values (ZJC: -9.2±0.4‰, n=48; FX: -9.7±0.5‰, n=79).

We then compare the measured $^{18}O_c$ against three commonly used proxies for the summer monsoon intensity – MS, carbonate content, and $^{13}C_c$. As the most iconic indicator of the East Asian summer monsoon intensity, MS is primarily governed by the abundance of nanoscale magnetite formed under soil wetting/drying oscillations (Ahmed and Maher, 2018), with high MS reflecting intense monsoonal rainfall (e.g. interglacial episodes) and vice versa. The carbonate minerals (including calcite and dolomite) are also sensitive to rainfall amount, with lower content under higher rainfall due to enhanced leaching (Meng et al., 2015). Previous studies treated $^{13}C_c$ as a proxy of local vegetation (i.e. C_3 and C_4 plants) on the CLP (Ding and Yang, 2000), assuming that CO_2 sourced from soil respiration dominates over atmospheric CO_2 in the soil pore system (Cerling et al., 1989). However, recent work shows that in the CLP region characterized by constant water deficiency, the ^{13}C is mainly governed by region aridity in response to monsoonal rainfall amount, with lower ^{13}C under high rainfall (Da et al., 2020).

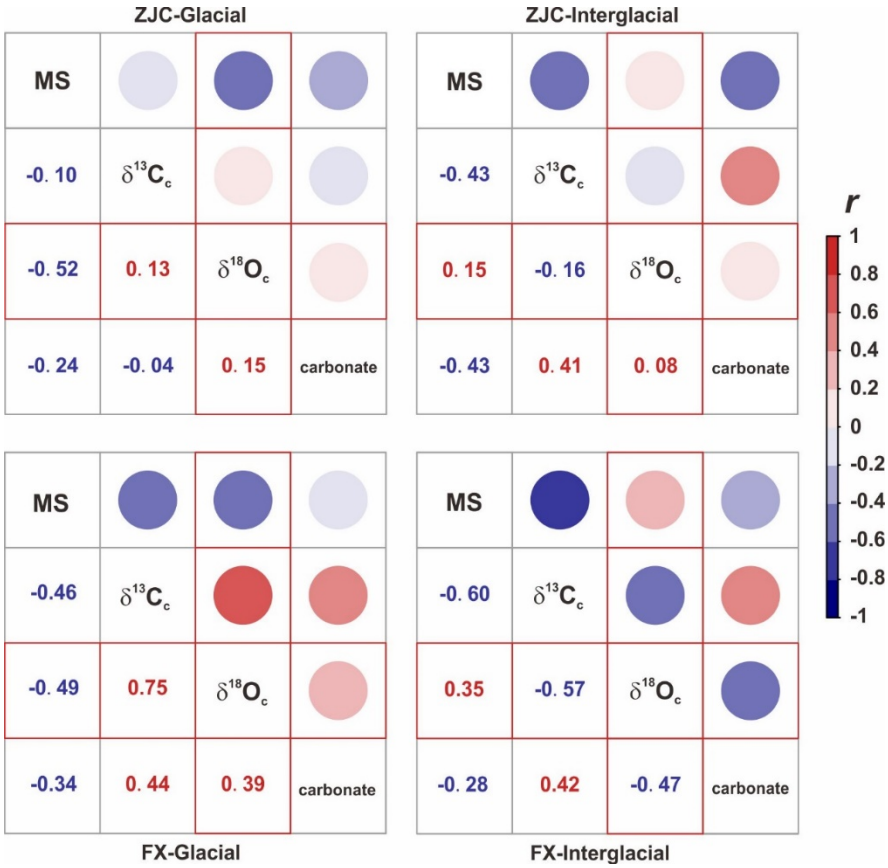

Figure 4. Correlation matrix plots of $^{18}O_c$ versus summer monsoon proxies during glacial and interglacial episodes. Blue and red colors denote negative and positive correlations, respectively. The shades of color indicate the degree of correlation. Numbers in the figure represent the correlation coefficient *r*.

We generate a Pearson correlation matrix to examine the relations between $^{18}O_c$ and summer monsoon proxies during glacial cycles and obtain consistent results between the two studied sections (Figure 4). In general, the glacial $^{18}O_c$ show positive correlations with the $^{13}C_c$ and carbonate content, and a negative correlation with the MS, implying more negative $^{18}O_c$ under higher rainfall, whereas the interglacial $^{18}O_c$ reveal opposite trends, meaning more positive $^{18}O_c$ under higher rainfall (Figure 4).

3.3.3. Glacial-interglacial $^{18}O_c$-rainfall correlations explained by pedogenic carbonate seasonality

We interpret the nonunique relationships between Quaternary $^{18}O_c$ and summer monsoon proxies as shifts in the timing of pedogenic carbonate growth. In the glacial periods, the weak summer monsoon limited rainfall events within the

growing season, making $^{18}O_c$ dominated by the growing-season $^{18}O_p$ and resulting in the negative correlation between $^{18}O_c$ and rainfall intensity as seen for the growing season (Figures 2a and 2c). During the interglacial episodes, the intensified monsoon likely facilitated more rainfall events in the non-growing season (Figure S2), leading to a prolonged carbonate-formation timespan with enhanced contributions from the non-growing season (Kelson, 2019). In this scenario, the $^{18}O_c$ could be imprinted by non-growing-season $^{18}O_c$, causing a positive correlation between $^{18}O_c$ and rainfall intensity, given (1) the positive $^{18}O_p$ – $^{18}O_c$ correlation (Figure 2b), (2) the positive non-growing-season $^{18}O_p$ – rainfall correlation (Figure 2d), and (3) the incorporation of non-growing season $^{18}O_p$ into $^{18}O_c$ (Section 3.1.3). Thus, the changes in the timing of pedogenic carbonate growth driven by summer monsoon intensity provide a plausible explanation for the observed correlations between $^{18}O_c$ and summer monsoon proxies.

The glacial-interglacial $^{18}O_c$ – rainfall patterns are consistent with the depth-dependent seasonality of pedogenic carbonate growth shown by the HYDRUS-1D model (Section 3.1.3). Because of the intense summer monsoon during interglacial episodes, carbonate minerals in most parts of the S_i paleosol units are completely leached away (Figure S6), resulting in deep Bk horizons sometimes penetrating the underlying glacial L_i units. In this case, the interglacial samples were selected from the upper or bottom part of the Bk horizon, and their $^{18}O_c$ reflect $^{18}O_p$ signals from the non-growing season or a mixture of growing and non-growing seasons, displaying a relatively weaker correlation between $^{18}O_c$ and MS compared to the glacial samples ($r = 0.15/0.35$ vs. -0.52/-0.49) (Figure 4).

4. Conclusions and Implications

We demonstrate a strong seasonality in pedogenic carbonate systems on the CLP across modern and glacial-interglacial timescales by combining modern data, modeling efforts, and ^{18}O geochemistry of Quaternary samples. Consistent with previous studies (Breecker et al., 2009; Huth et al., 2019), our results demonstrate the primary control of rainfall infiltration events on soil carbonate growth and associated seasonality. In the East Asian summer monsoon domain, such seasonality could translate into distinct trends between $^{18}O_c$ and rainfall proxies, providing additional insights into past summer monsoon changes. For instance, $^{18}O_c$ increase concomitantly with MS during the warm intervals of the underlying Miocene-Pliocene red-clay formation (e.g. the Pliocene warm period: *ca.* 5-3 Myr, the Mid-Miocene Climate Optimum: 17.0-14.5 Myr) (Dong et al., 2018; Kaakinen et al., 2006), implying a strong summer monsoon comparable to the interglacial episodes. Moreover, it has been challenging to reconstruct glacial climate conditions with the weak summer monsoon, due to the interference from detrital materials and the lack of reliable archives (An et al., 2014; Sun et al., 2006). Based on our results (e.g. the good correlations between monsoon proxies

and $^{18}O_c$, Figure 4), we propose that pedogenic carbonates (e.g. FDC) are a convincing archive for inferring environmental conditions in the glacial periods. Overall, our work provides a promising method to constrain the seasonality of soil carbonates, advancing our understanding of their paleoenvironmental implications.

Acknowledgments

This work is funded by the National Science Foundation of China (No. 41991321 to J. Ji, No. 42102228 to J. Da), the Fundamental Research Funds for the Central Universities (No. 14380112 to J. Da), and the fellowship of China Postdoctoral Science Foundation (No. 2021M691493 to J. Da). G.K. Li thanks support from a UCSB Regents Junior Faculty Fellowship.

Data Availability Statement

All the additional information and data sets supporting the conclusions are available online, including Text S1–S3, Figures S1–S6, Table S1 in Supporting Information S1, and Data Sets S1 and S2 in the online data repository Figshare (https://doi.org/10.6084/m9.figshare.19353182.v1).

References

An, Z., Sun, Y., Chang, H., Zhang, P., Liu, X., Cai, Y., et al. (2014). Late Cenozoic climate change in monsoon-arid Asia and global changes. In *Late Cenozoic Climate Change in Asia* (pp. 491–581). Springer.Araguás-Araguás, L., Froehlich, K., & Rozanski, K. (1998). Stable isotope composition of precipitation over southeast Asia. *Journal of Geophysical Research: Atmospheres*, *103*(D22), 28721–28742. https://doi.org/10.1029/98JD02582Barta, G. (2011). Secondary carbonates in loess-paleosoil sequences: a general review. *Open Geosciences*, *3*(2). https://doi.org/10.2478/s13533-011-0013-7Beverly, E. J., Levin, N. E., Passey, B. H., Aron, P. G., Yarian, D. A., Page, M., & Pelletier, E. M. (2021). Triple oxygen and clumped isotopes in modern soil carbonate along an aridity gradient in the Serengeti, Tanzania. *Earth and Planetary Science Letters*, *567*, 116952. https://doi.org/10.1016/j.epsl.2021.116952Breecker, D. O., Sharp, Z. D., & McFadden, L. D. (2009). Seasonal bias in the formation and stable isotopic composition of pedogenic carbonate in modern soils from central New Mexico, USA. *Geological Society of America Bulletin*, *121*(3–4), 630–640. https://doi.org/10.1130/b26413.1Caves, J. K., & Chamberlain, C. P. (2018). The evolution of hydroclimate in Asia over the Cenozoic: A stable-isotope perspective. *Earth-Science Reviews*.Caves, J. K., Moragne, D. Y., Ibarra, D. E., Bayshashov, B. U., Gao, Y., Jones, M. M., et al. (2016). The Neogene de-greening of Central Asia. *Geology*, *44*(11), 887–890.Cerling, T. E. (1999). Stable carbon isotopes in palaeosol carbonates. *Palaeoweathering,*

Palaeosurfaces and Related Continental Deposits, 43–60.Cerling, Thure E., & Quade, J. (1993). Stable Carbon and Oxygen Isotopes in Soil Carbonates. *Climate Change in Continental Isotopic Records*, *78*, 217–231.Cerling, Thure E., Wynn, J. G., Andanje, S. A., Bird, M. I., Korir, D. K., Levin, N. E., et al. (2011). Woody cover and hominin environments in the past 6 million years. *Nature*, *476*(7358), 51–56. https://doi.org/10.1038/nature10306Da, J., Zhang, Y. G., Wang, H., Balsam, W., & Ji, J. (2015). An Early Pleistocene atmospheric CO2 record based on pedogenic carbonate from the Chinese loess deposits. *Earth and Planetary Science Letters*, *426*, 69–75.Da, J., Zhang, Y. G., Li, G., Meng, X., & Ji, J. (2019). Low CO2 levels of the entire Pleistocene epoch. *Nature Communications*, *10*(1), 4342. https://doi.org/10.1038/s41467-019-12357-5Da, J., Zhang, Y. G., Li, G., & Ji, J. (2020). Aridity-driven decoupling of 13C between pedogenic carbonate and soil organic matter. *Geology*. https://doi.org/10.1130/G47241.1Dansgaard, W. (1964). Stable isotopes in precipitation. *Tellus*, *16*(4), 436–468.Ding, Z. L., & Yang, S. L. (2000). C3/C4 vegetation evolution over the last 7.0 Myr in the Chinese Loess Plateau: evidence from pedogenic carbonate 13C. *Palaeogeography, Palaeoclimatology, Palaeoecology*, *160*(3–4), 291–299.Dong, J., Liu, Z., An, Z., Liu, W., Zhou, W., Qiang, X., & Lu, F. (2018). Mid-Miocene C4 expansion on the Chinese Loess Plateau under an enhanced Asian summer monsoon. *Journal of Asian Earth Sciences*, *158*, 153–159.Drever, J. I. (1982). The geochemistry of natural waters.Fischer-Femal, B. J., & Bowen, G. J. (2021). Coupled carbon and oxygen isotope model for pedogenic carbonates. *Geochimica Et Cosmochimica Acta*, *294*, 126–144. https://doi.org/10.1016/j.gca.2020.10.022Hu, Q., Wang, X., Yi, S., Meng, X., Long, H., Vandenberghe, J., et al. (2018). The paleoclimatic implication of oxygen isotopes of authigenic carbonates in loess on the Northeastern Tibetan Plateau since Last Glacial Maximum. *Progress in Physical Geography: Earth and Environment*, *42*(6), 826–840. https://doi.org/10.1177/0309133318803021Huth, T. E., Cerling, T. E., Marchetti, D. W., Bowling, D. R., Ellwein, A. L., & Passey, B. H. (2019). Seasonal Bias in Soil Carbonate Formation and Its Implications for Interpreting High-Resolution Paleoarchives: Evidence From Southern Utah. *Journal of Geophysical Research: Biogeosciences*, *124*(3), 616–632.Kelson, Julia R., Huntington, K. W., Breecker, D. O., Burgener, L. K., Gallagher, T. M., Hoke, G. D., & Petersen, S. V. (2020). A proxy for all seasons? A synthesis of clumped isotope data from Holocene soil carbonates. *Quaternary Science Reviews*, *234*, 106259. https://doi.org/10.1016/j.quascirev.2020.106259Kelson, Julia Rae. (2019). *Terrestrial Paleoclimate of the Cenozoic: Insights from and Developments of the Soil Carbonate Clumped Isotope Thermometer*.Lee, J.-E., Risi, C., Fung, I., Worden, J., Scheepmaker, R. A., Lintner, B., & Frankenberg, C. (2012). Asian monsoon hydrometeorology from TES and SCIAMACHY water vapor isotope measurements and LMDZ simulations: Implications for speleothem climate record interpretation. *Journal of Geophysical Research: Atmospheres*, *117*(D15). https://doi.org/10.1029/2011JD017133Li, G., Chen, J., & Chen, Y. (2013). Primary and secondary carbonate in Chinese loess discriminated by trace element composition. *Geochimica Et*

Cosmochimica Acta, *103*, 26–35.Li, T., & Li, G. (2014). Incorporation of trace metals into microcodium as novel proxies for paleo-precipitation. *Earth & Planetary Science Letters*, *386*(1), 34–40.Licht, A., Dupont-Nivet, G., Meijer, N., Caves Rugenstein, J., Schauer, A., Fiebig, J., et al. (2020). Decline of soil respiration in northeastern Tibet through the transition into the Oligocene icehouse. *Palaeogeography, Palaeoclimatology, Palaeoecology*, *560*, 110016. https://doi.org/10.1016/j.palaeo.2020.110016Lyu, S., Wang, J., Song, X., & Wen, X. (2021). The relationship of D and 18O in surface soil water and its implications for soil evaporation along grass transects of Tibet, Loess, and Inner Mongolia Plateau. *Journal of Hydrology*, 126533. https://doi.org/10.1016/j.jhydrol.2021.126533Meng, X., Liu, L., Balsam, W., Li, S., He, T., Chen, J., & Ji, J. (2015). Dolomite abundance in Chinese loess deposits: A new proxy of monsoon precipitation intensity. *Geophysical Research Letters*, *42*(23).Meng, X., Liu, L., Wang, X. T., Balsam, W., Chen, J., & Ji, J. (2018). Mineralogical evidence of reduced East Asian summer monsoon rainfall on the Chinese loess plateau during the early Pleistocene interglacials. *Earth and Planetary Science Letters*, *486*, 61–69.Meyer, N. A., Breecker, D. O., Young, M. H., & Litvak, M. E. (2014). Simulating the Effect of Vegetation in Formation of Pedogenic Carbonate. *Soil Science Society of America Journal*, *78*(3). https://doi.org/10.2136/sssaj2013.08.0326Milliere, L., Spangenberg, J. E., Bindschedler, S., Cailleau, G., & Verrecchia, E. P. (2011). Reliability of stable carbon and oxygen isotope compositions of pedogenic needle fibre calcite as environmental indicators: examples from Western Europe. *Isotopes Environ Health Stud*, *47*(3), 341–58. https://doi.org/10.1080/10256016.2011.601305Ringham, M. C., Hoke, G. D., Huntington, K. W., & Aranibar, J. N. (2016). Influence of vegetation type and site-to-site variability on soil carbonate clumped isotope records, Andean piedmont of Central Argentina (32–34°S). *Earth and Planetary Science Letters*, *440*, 1–11. https://doi.org/10.1016/j.epsl.2016.02.003Sheng, X., Chen, J., Ji, J., Chen, T., Li, G., & Teng, H. H. (2008). Morphological characters and multi-element isotopic signatures of carbonates from Chinese loess–paleosol sequences. *Geochimica Et Cosmochimica Acta*, *72*(17), 4323–4337. https://doi.org/10.1016/j.gca.2008.06.024Simunek, J., Van Genuchten, M. T., & Sejna, M. (2005). The HYDRUS-1D software package for simulating the one-dimensional movement of water, heat, and multiple solutes in variably-saturated media. *University of California-Riverside Research Reports*, *3*, 1–240.Sun, Y., Clemens, S. C., An, Z., & Yu, Z. (2006). Astronomical timescale and palaeoclimatic implication of stacked 3.6-Myr monsoon records from the Chinese Loess Plateau. *Quaternary Science Reviews*, *25*(1–2), 33–48.Wang, K., Lu, H., Garzione, C. N., Zhao, L., Liang, C., Li, S., et al. (2022). Enhanced soil respiration, vegetation and monsoon precipitation at Lantian, East Asia during Pliocene warmth. *Climate Dynamics*. https://doi.org/10.1007/s00382-022-06243-yWang, Y., Cheng, H., Edwards, R. L., Kong, X., Shao, X., Chen, S., et al. (2008). Millennial- and orbital-scale changes in the East Asian monsoon over the past 224,000 years. *Nature*, *451*(7182), 1090–1093. https://doi.org/10.1038/nature06692Yang, J., Chen, J., An, Z., Shields, G., Tao, X., Zhu, H., et al. (2000). Variations in 87Sr/86Sr ratios of calcites in

Chinese loess: a proxy for chemical weathering associated with the East Asian summer monsoon. *Palaeogeography, Palaeoclimatology, Palaeoecology*, *157*(1–2), 151–159.Yang, S., Ding, Z., Wang, X., Tang, Z., & Gu, Z. (2012). Negative 18O– 13C relationship of pedogenic carbonate from northern China indicates a strong response of C3/C4 biomass to the seasonality of Asian monsoon precipitation. *Palaeogeography, Palaeoclimatology, Palaeoecology*, *317*, 32–40.Zamanian, K., Pustovoytov, K., & Kuzyakov, Y. (2016). Pedogenic carbonates: Forms and formation processes. *Earth-Science Reviews*, *157*, 1–17.Zhang, Z., Li, G., Yan, H., & An, Z. (2018). Microcodium in Chinese loess as a recorder for the oxygen isotopic composition of monsoonal rainwater. *Quaternary International*, *464*, 364–369. https://doi.org/10.1016/j.quaint.2017.10.050Zhao, W., Sun, Y., Balsam, W., Zeng, L., Lu, H., Otgonbayar, K., & Ji, J. (2015). Clay-sized Hf-Nd-Sr isotopic composition of Mongolian dust as a fingerprint for regional to hemispherical transport. *Geophysical Research Letters*, *42*(13), 5661–5669. https://doi.org/10.1002/2015GL064357